Metal Binding Peptides for Separation and Concentration in Hydrometallurgy

John Taylor Hamann

A thesis
submitted in partial fulfillment of the
requirements for the degree of

MASTER OF SCIENCE

University of Washington
2021

Committee:
Lucien Brush
Joyce Cooper

Program Authorized to Offer Degree:
Materials Science & Engineering | College of Engineering

University of Washington

Abstract

Metal Binding Peptides for Separation and Concentration in Hydrometallurgy

John Taylor Hamann

Chair of the Supervisory Committee:
Lucien Brush
Department of Materials Science & Engineering

Strong solid binding peptides selected through biopanning methods sometimes show precipitating activity in solutions containing specific inorganic precursors. Material specificity of these peptides could offer selective precipitation as an alternative method in metal extraction and separation. While a majority of peptide guided biomineralization studies focus on improving molecular assembly and synthesis of nanoscale materials, few have considered the potential for selectively precipitating metals and compounds from complex solutions. The goal of this work is to explore relevant literature and investigate precipitation activity of two metal binding peptides l-AuBP1 and l-AgBP1 for Au and Ag particles in the absence of reducing agents. In triplicate UV-Vis studies at room temperature, l-AuBP1 triggered formation of solid Au, but not Ag particles while l-AgBP1 formed neither. Furthermore, oxidation of l-AuBP1, confirmed through mass spectrometry, indicates molecular degradation limiting its potential use in biomining applications.

Contents

Figures

Tables

Introduction

Biological approaches to metal extraction and separation offer unique opportunities to mitigate current issues in hydrometallurgy and improve process sustainability. The next generation of biotechnology in metals separation focuses on high molecular and ionic selectivity found in protein and peptide molecules. The sequence-based architecture of peptides enables a wide range of chemical and steric configurations allowing complex interactions in aqueous environments. Development and design of genetically engineered peptides for inorganics (GEPIs) has uncovered a trove of sequences demonstrating strong binding affinity to many material surfaces (Tamerler et al., 2007). Remarkably, a subset of these peptides control precipitation for various inorganic species with similar functionality to natural mineralizing proteins (Dickerson et al., 2008). Peptide guided biomineralization could provide a novel mechanism to enhance selective precipitation methods for separation and concentration processes in hydrometallurgy.

Aqueous metal separations currently utilize a wide range of processes such as solvent extraction, ion exchange, activated carbon adsorption, ultrafiltration, and precipitation. These processes are often environmentally intensive requiring the use of organic solvents, synthetic resins, and highly caustic reagents (Free, 2013). The manufacturing, use, and disposal of these materials contribute significant environmental impacts like terrestrial and freshwater acidification to the production of metal products (Vahidi & Zhao, 2017). Offering alternatives to these brute force methods could allow for more environmentally responsible metal processing. The success of commercial bioleaching and biooxidation in providing more economically and environmentally sustainable processes establishes a foundation for new biotechnology in metals separation (Johnson, 2013).

Design and discovery of proteins and peptides for metals separation has made exciting progress in the past two decades with a large focus on biosorption through increasing the selectivity of protein-ion binding interactions (Mattocks & Cotruvo, 2020). In parallel, a smaller effort has focused on using the mechanisms of biomineralization to achieve enhanced selectivity in precipitation by triggering formation of specific

insoluble species (Hatanaka et al., 2017 & Tomizaki et al., 2020). This report focuses on developing the latter method using short peptides with strong binding affinity to metal surfaces.

Background

Definitions

Biomineralization refers to the process by which living organisms produce mineral crystals through biological means. In this study we consider the ability for short peptides guiding or catalyzing the formation of any inorganic species to fall under this definition.

Biomining refers primarily to the use of microorganisms aiding in the extraction of metals from surrounding media which can be used for recovering economically valuable metals or used in bioremediation. Biomining serves as an umbrella term which traditionally covers the more specific processes like bioleaching and biooxidation.

Bioleaching typically involves the use of iron oxidizing bacteria which yield soluble metal ions. The role of the microorganism is the further oxidation of the ore through regeneration of chemical oxidant.

Biooxidation in contrast to bioleaching, is an oxidation process caused by microbes whereby the target metal is enriched within the solid phase rather than being solubilized. This is accomplished through selective dissolution of gangue mineral by microbes.

Biosorption refers mostly to the capabilities of biomass to accumulate heavy metals or other contaminants from wastewater streams. More recently however, this refers to the capabilities of specific microorganisms or specific proteins to chelate metal ions to aid in separation and concentration processes of soluble metals.

GEPI is an abbreviation for Genetically Engineered Peptides for Inorganics.

GEPIs

Taking inspiration from natural proteins governing the formation of biological hard tissues, Molecular Biomimetics (Sarikaya et al., 2003) offers nanotechnology through biology utilizing genetically engineered peptides for inorganics (GEPI). These peptides offer a new set of tools for enhancing nanotechnology by providing molecular specificity for inorganic surfaces allowing new types of functionalization, molecular templating, and importantly influence over solution mineralization. Peptides with synthesizing capabilities have been found using directed evolution techniques for an increasingly wide range of inorganic materials (Dickerson et al., 2008).

Biopanning, a technique for selecting peptides with binding affinities to a specific target, is a common method employed against inorganic surfaces. Random peptide libraries are available in sequence lengths between 7 and 15 amino acids with varying types of residue expression profiles and physical configurations. Random peptide libraries often utilize cell surface display or phage display platforms coupling peptide functionality and genetic encoding to recover the amino acid sequences following the selection process. In the selection process, random peptide libraries are first incubated with a target material followed by several rounds of selective pressure such as stringent washing or ultrasonic vibration to enrich the pool of strong binders (Donatan et al., 2009). After identifying the peptide sequences from the strong binding pool, further characterization of peptide binding affinities using more quantitative techniques are carried out to determine molecular binding strengths. Insight gleaned from resulting solid binding peptide libraries supports rational design of engineered sequences for enhanced functionality (Oren et al., 2007).

Potential and current applications of strong inorganic binding peptides have been found in new biosensor architectures (Khatayevich et al., 2014), patterning of quantum dots (Zin et al., 2007), implant coatings (Yazici et al., 2013), and regenerative dental therapeutics (Dogan et al., 2018) among many others. The applications of strong binding peptides in biomining remains a relatively unexplored area and thus motivates the current work to explore functionality relevant to metals separation. The following sections of

the background will discuss the concept of selective precipitation and focus on biomineralizing peptides with relevant functionality.

Selective Precipitation

Within the discipline of hydrometallurgy (Free, 2013), the use of selective precipitation is a common method for separating dissolved metals. Fundamentally, the selectivity is driven by differences in solubility as a function of pH. These differences in solubility are used to trigger precipitation of specific metal containing species while keeping other metals dissolved thus facilitating separation through a change in phase. Precipitation occurs when the product of the reactant activities exceeds the solubility product (K_{sp}). The excess ions transition into solid precipitates reducing ion activities until the solubility product is reached and the solution comes to equilibrium. When the product of the reactant activities is below K_{sp}, precipitates existing in solution will dissolve if the reaction is reversible.

Traditional methods for altering reactant activities include changing the temperature and pressure. The activity of ions in solution is primarily driven by concentration in ideal solutions, however most solutions are non-ideal. For example, because ions tend to interact with each other in solution, increases in ionic strength can decrease the activity of a particular ion. Similarly, a peptide or protein could form favorable interactions with precursor ions thereby lowering their activities in solution. Alternatively, a peptide could interact favorably with a solid species decreasing its activity. In the latter example the peptide could inhibit a dissociation reaction and promote nucleation. However, strong surface adsorption to particles may prohibit further growth of nuclei.

Literature Review

The body of research discussing the biomineralizing activity of various peptides and proteins is quite expansive. A quick search on Google Scholar with the terms “peptide” and “biomineralization” yields over 16,000 results for publications between the years of 2000 and 2021. About half of these results were published in the last 5 years. (Search conducted on November 19, 2021, not including citations). While

providing a rich source of background information, the diverse vocabulary stemming from various research perspectives presents a complicating factor for narrowing down relevant results. The use of other functional descriptors like peptide based -synthesis, -formation, -precipitation, and -crystallization further complicates this search. Articles discussing selective precipitation by peptides also tend to discuss other functionalities relevant for directing nanoscale synthesis which can be difficult to filter out. These obstacles have prompted a more ad hoc approach for identifying relevant literature.

This mini review will discuss several examples of specific peptides triggering selective precipitation with two distinct characteristics. 1) Peptides demonstrating selectivity for one inorganic species over another in precipitation and 2) Peptides which precipitate species in nonequilibrium conditions or without traditional reducing agents. The review will discuss how the peptides were selected, the conditions demonstrating precipitation activity, the proposed mechanism, and key features of the sequence. The literature search process involved specific Google scholar search terms and following citations in related works.

Google Scholar search terms used:

1. "peptide" "selective" "nonequilibrium" "separation" "precipitation" OR "mineralization" OR "biomineralization" -disease -bacteria
2. "biopanning" "selective" "precipitation" "precursor" OR "mineralization" OR "biomineralization" -disease -bacteria -drug
3. “peptide" "selective" "metal" "recovery" "separation" "reduction" OR "precipitation" OR "mineralization" OR "biomineralization" OR "extraction" -disease -bacteria

Dai et al., (2005) presents a useful example of how strong binding peptides can induce precipitation for their selected target material. A Cu_2O binding peptide called CN225 (RHTDGLRRIAAR), previously selected using the FliTrx platform for high binding strength (Thai et al., 2004) was engineered into the permissive site of a DNA binding protein TraI. Templated growth of Cu_2O nanoparticles was accomplished using circular DNA to arrange the engineered protein. The precursor was 1M NaCl in an electrolytic cell

with copper cathode and anode configured to produce 6mM of Cu ions in the solution. Notably, formation of Cu_2O nanoparticles occurred under nonequilibrium conditions and only upon the inclusion of CN225. At 5% of the Cu_2O solubility product ($K_{sp} \approx 1.45 \times 10^{-15}$) transient nuclei form and spontaneously redissolve because the electrolyte is subsaturated with regard to the precursor ions. However, the authors found CN225 promotes the formation of stable Cu_2O nanoparticles even under these thermodynamically unfavorable conditions. They suggest that strong interfacial adsorption of CN225 stabilizes transient Cu_2O nuclei before redissolving. Because the peptide is material specific the authors claim that other transient nuclei would not receive the same energetic benefit under more complex conditions. The amino acids and motifs implicated in the strong binding of CN225 are discussed in (Thai et al., 2004). Analysis of the Cu_2O binders found enrichment of tryptophan, glycine, methionine, and arginine and depletion in leucine, tyrosine, proline, serine, and threonine. CN225 is hydrophilic, highly basic, has a net charge of +3, and contains twin arginine residues. Initially pairs of arginine (R) residues in RXXR and RR sequence configuration were thought to be significant in binding activity. However, a follow up study indicates cyclic peptide conformation plays a more important role than short amino acid motifs in the binding activity of CN225 to Cu_2O inorganic surfaces (Choe et al., 2007)

Note: Dai et al., (2005) is one example of relevant literature which describes peptide guided precipitation without using "biomineralization" terminology.

Fang et al. (2008) demonstrate a novel subtractive biopanning method used to identify peptides which induce the formation of titania (TiO_2), but not silica (SiO_2) using a 12 AA length phage display peptide library. Unlike traditional biopanning selection, this subtractive method involved first removing silica binding phages and selecting the remainder for titania binding activity. Ti(~~Si~~)-1 (YPSAPPQWLTNT) was found in half of the remaining phage colonies following selection. Precipitation experiments were carried out at room temperature for 10 minutes over a range of pH in a 80 mM phosphate-citrate buffer containing either 80mM silicic acid or 40 mM potassium bis(oxalato)oxotitanate(IV) as silica and titania precursors respectively.

Precipitation activity was compared to positive and negative control peptides with known activity. The positive control, recombinant silaffin C (Kröger et al., 2006), is known to form both silica and titania under these conditions. The negative control is a basic peptide (LFTVGMKPSPRP) known to lack silica and titania precipitation activity. Ti(~~Si~~)-1 did not induce silica formation over a pH range of 3-8 within the allowed 10 minute incubation time and showed the highest titania precipitation among those evaluated. Ti(~~Si~~)-1 showed bimodal precipitation activity of titania relative to its isoelectric point (5.5) with higher precipitation rates between pH 3 and 5 and reduced above pH 6.

While the authors do not discuss the precise mechanism of formation, they suggest that the positive charge of the peptide at low pH may allow for enhanced electrostatic assembly of anionic oxalatotitanium complexes. The titania selective precipitating peptides identified in this study show key differences from peptides with known silica and titania binding activity. Peptides with strong silica precipitation activity had strong enrichment of histidine residues, enrichment of hydroxyl-containing residues, and high cationic charge (Knecht & Wright, 2003). Peptides with high titania precipitating activity had enrichment of basic residues. In contrast, the Ti(~~Si~~) peptides showed depletion of basic residues, slight enrichment of hydroxyl-containing residues, and few histidine residues.

Hatanaka et al. (2017) describes the rational design of mineralizing peptides for the recovery of rare earth elements. Lanthanide mineralizing peptides (Lamp) were selected for binding affinity to hydroxylated Nd_2O_3 nanoparticles (<100nm) using the T7 phage display system. In their selection process they used the NNK codon to generate a library with high hydrophilic amino acid composition. Cyclic peptide configurations were employed to reduce unfavorable changes in conformational entropy for improved target recognition. Hydroxylated nanoparticles were chosen to increase the binding preference of selected peptides to hydroxyl groups with the rational of shifting speciation of Ln^{3+} ions in favor of insoluble lanthanide-hydroxide complexes by limiting dehydroxylation at neutral and slightly acidic pH.

One selected peptide Lamp-1 (SCLWGDVSELDFLCS) demonstrates exceptional selective mineralization activity in a variety of conditions. Lamp-1 triggered precipitation of $Dy(NO_3)_3$ (aqueous) into $Dy(OH)_3$

(solid) in a variety of buffers and was also observed for Dy chloride and acetate salts. In contrast, previously identified lanthanide ion binding peptides (LBT3, RE-1, and NC1) showed no mineralizing activity. Mineralization studies of the lanthanide (Ln) series with Lamp-1 indicated selective precipitation for heavy Ln species over light Ln species correlating with the stability constants of the respective Ln-hydroxides. Lamp-1 precipitation was successful even in synthetic seawater where spectator cation (Na^+, Mg^{2+}, K^+ and Ca^{2+}) concentrations were 160-times higher than Dy^{3+}. XAFS analysis of the precipitates indicated amorphous particles containing both $Dy(OH)_3$ and Lamp-1 peptide.

Hatanaka et al.'s proposed mechanism describes Lamp-1 weakly recognizing Ln^{3+} through electrostatic interactions, Ln-hydroxide generation by acidic residues, stabilization of Ln-hydroxide through complexation with Lamp preventing dehydroxylation/rehydration. Hydrophobic accumulation of the Ln-hydroxide-Lamp complex then leads to precipitation. The release of coordinating water molecules from Ln^{3+} is entropically favorable enough to overcome the reduced conformational entropy of the peptide upon stabilization of the complex. Charge neutralization helps facilitate spontaneous accumulation and precipitation.

In Hatanaka et al.'s discussion they point out key differences between mineralizing peptides with sophisticated control over metal crystal morphology and those forming amorphous precipitates. In the former, molecular recognition of the crystallographic surface and strong affinity are significant functions for controlling the crystal growth of nanoscale metal particles. In the latter, ion interaction and hydrogen bond formation play important roles in regulating the precipitation activity of amorphous metal-hydroxide-organic composites. Use of reducing agents is often used to accelerate the precipitation process in concert with solid binding peptides to influence the morphology, however selective mineralization by peptides requires a more targeted approach to limit the formation of unwanted species.

Tomizaki et al. (2020) describes selective reduction of $HAuCl_4$ in mixed solutions containing H_2PtCl_6 using nonnatural aromatic amino acid-containing peptides. Their work focuses on a β-sheet forming peptide (RU006: Ac-AIAKAXKIA-NH2, X = L-2-naphthylalanine, NaI) used in a previous study to form gold

nanoribbons (Tomizaki et al., 2014). RU006 was *de novo* designed to form β-sheet structure through hydrophobic interactions with Isoleucine (I) residues and facilitate π-π stacking with an aromatic NaI residue driving peptide self-assembly in solution. Lysine (K) residues were inserted to facilitate greater solubility and accommodate $AuCl_4^-$ ions in the hydrophobic interior of the assembled peptide nanostructure. Two other peptides (NaI^2)-RU006 and (Ant^6)-RU006, were created to increase aromatic electron availability by substituting an additional NaI residue in position two and by substituting the original NaI residue with an Anthracene containing residue.

In their 2020 study, Tomizaki et al. prepared mixed solutions of $HAuCl_4$ and H_2PtCl_6 (0.05mM each) and observed reactions with peptides at 0.2mM concentration. Reduction of metals with peptides were carried out at 40°C in a temperature-controlled heat block for 24 hours in the dark. Selectivity was determined by measuring the composition of solid particles following the reaction. They found that Anthracene (Ant) containing peptides selectively reduced $HAuCl_4$ over H_2PtCl_6 more so than peptides containing either one or two NaI residues. Aromatic rings of the peptide donate electrons to $AuCl_4^-$ in reduction to $Au_{(s)}$. NaI residues can donate two electrons while the Ant residue can provide four electrons with a total of three electrons needed to fully reduce $AuCl_4^-$.

Their results show that (Ant^6)-RU006 peptide triggered quick formation of gold particles early in the reaction followed by platinum particle formation to a lesser extent. Because Ant containing peptides could provide three electrons to fully reduce $AuCl_4^-$, the need for multiple peptide monomer participation could be avoided. The two naphthene rings in (NaI^2)-RU006 seemed to disrupt the self-assembly process which resulted in more promiscuous reduction of H_2PtCl_6. Comparisons with sodium borohydride and ascorbic acid reducing agents indicated lower degrees of selectivity compared to the (Ant^6)-RU006 peptide. They found none of the peptides reduced H_2PtCl_6 in the absence of $HAuCl_4$ and found that formation of Au(I) intermediates aided in the reduction of H_2PtCl_6. Thus, rapid reduction of $HAuCl_4$ contributes to observed selectivity through inhibition of intermediate Au(I) formation.

Unique peptide-ion complexation appears to be an important mechanism for initiating and catalyzing the formation of insoluble species from soluble ionic form. As demonstrated by Hatanaka et al. (2017), ion binding and metal binding functions alone do not confer precipitation activity. Congruent orchestration of multiple ions by peptides coupled with moderate peptide surface adsorption seems to be necessary for balancing ionic dehydration, charge neutralization, and enthalpic adsorption with decreased conformational entropy upon adsorption. In addition to sequence and amino acid composition, peptide conformation plays a critical role in the interactions with inorganic surfaces. In the context of selective metal reduction, electron availability can play a significant role in preventing the formation of disruptive intermediaries while surface interactions seem to play a larger role in resulting morphology.

Experimental Work

This work aims to explore the selectivity of strong metal binding peptides to precipitate metal ions for which they were selected. Due to resource limitations on this work, only two peptides (l-AuBP1 and l-AgBP1) were chosen for an initial exploration into peptide guided selective precipitation. Gold and silver were selected as the target products because the peptides which bind to them are well characterized and distinct characteristic UV-Vis spectra are observed upon the formation of Au and Ag nanoparticles in solution.

Gold binding peptide l-AuBP1 (WAGAKRLVLRRE) was derived by Hnilova et al. in 2008 using a FliTrx random peptide display library with five rounds of binding selection on polycrystalline Au foil. The 2008 study points out the distinct lack of histidine and cysteine amino acids in l-AuBP1 indicating a novel binding mechanism. Circular dichroism spectra of l-AuBP1 indicate random coil structure and helical polyproline type II secondary structures. The conformational flexibility of l-AuBP1 indicated by the random coil structure likely allows for adaptability when adsorbing to gold surfaces. In unpublished work, Hnilova et al. found l-AuBP1 reduced gold ions under ambient conditions suggesting that peptide ion complexation

catalyzes Au crystal formation. A handful of amino acids known to facilitate Au reduction and nanoparticle formation (W, Y, K, R, and C) (Slocik et al., 2005) are present in l-AuBP1.

Silver binding peptides l-AgBP1 (TGIFKSARAMRN) and l-AgBP2 (EQLGVRKELRGV) (Hnilova et al., 2012) were selected from a group of strong silver binding peptides selected using a FliTrx random peptide display library against silver surfaces. The sequences from the final round of biopanning were compared to sequences derived for gold foil using a similarity score to identify peptides with low sequence similarity to gold binding peptides (Oren et al., 2007). In the 2012 study by Hnilova, investigation of relative binding strengths using SPR of the circular forms (-C) of AgBP1 and AgBP2 on gold and silver surfaces indicated preferential adsorption to silver surfaces over gold. Adsorption curves for AgBP1C revealed significant adsorption to Ag with moderate adsorption to Au. Similarly, AgBP2C showed high adsorption to Ag surfaces and very low adsorption to Au surfaces. In a study conducted around the same time, AgBP2 was integrated into a periplasmic protein to engineer silver tolerance into E. coli (Sedlak et al., 2012). Upon exposure to silver nitrate solution, crystalline silver nanoparticles formed in the periplasm of the engineered E. coli reducing the toxic effects of the free Ag^{+} ions in the environment.

Linear AuBP1 (WAGAKRLVLRRE) was chosen for studying selective Au precipitation because of its known precipitating activity and strong binding. Linear AgBP1 (TGIFKSARAMRN) was selected to test Ag precipitation because of its strong Ag binding and low sequence similarity to AuBP1 binding (Oren et al., 2007), however its precipitating capabilities in the absence of auxiliary reducing agents remains to be experimentally observed. Chloroauric acid ($HAuCl_4$) and silver nitrate ($AgNO_3$) were selected as precursors for evaluating l-AuBP1 and l-AgBP1 guided precipitation.

Controlling pH

Controlling pH is a highly desirable experimental constraint to compare the precipitation activities of l-AuBP1 and l-AgBP1. Selection of a suitable buffering agent for both $HAuCl_4$ and $AgNO_3$ turned out to be a non-trivial task. Common biological buffers like HEPEs (Chen et al., 2010), MOPS (Chandra et al., 2017),

and TRIS (Chen et al., 2014) act as reducing agents for $HAuCl_4$ while phosphate buffer and bicarbonate buffer lead to the formation of insoluble species of silver phosphate and silver carbonate respectively. Through an iterative exploration of buffering agents, acetate buffer was found to be amenable for both $HAuCl_4$ and $AgNO_3$ avoiding a buffer side reaction. However, the useful pH of acetate buffer lies in the acidic range (3.6 – 5.6) precluding its use for stabilizing higher pH values. A high and low pH of 5.4 and 3.8 were selected as two controlled test conditions following a rule of thumb to keep the molar ratio between the weak acid (acetic acid) and its conjugate base (sodium acetate) within a tenfold ratio to ensure effectiveness.

Selectivity

The selection of $HAuCl_4$ and $AgNO_3$ do not represent realistic precursors for many separation and concentration processes and serve primarily as a platform for exploring a proof of concept. These precursors introduce limitations, ironically because Au^{3+} is easily reduced and Ag forms many insoluble salt precipitates. While the refinement of Au is an important hydrometallurgical practice (see Wohlwill process), selective precipitation of $HAuCl_4$ or $AgNO_3$ into solid species is a somewhat trivial process that occurred while identifying suitable buffering agents. Furthermore, mixture of $HAuCl_4$ and $AgNO_3$ produces $AgCl_{(s)}$ as a precipitate leaving the gold in solution. In light of this, experimental design focuses on peptide activity against individual precursors under different conditions rather than under mixed conditions.

Expected Observations

The presence of nanosized gold particles suspended in solution is expected to produce a characteristic peak in absorbance spectra near 560nm ± 50nm while nanosized silver particles suspended in a solution are expected to produce a characteristic peak near 420nm ± 50nm depending on size, shape, and functionalization (*UV-Vis Spectroscopy Open Source Reference Data Library for Nanoparticles*, 2021). The background spectra of $HAuCl_4$ is expected to produce a signature peak around 311nm (Peck et al. 1991). For solutions containing $AgNO_3$, an absorbance peak corresponding to Ag^+ ions is expected at

217nm which lies outside of the limits of the spectrophotometer (Tecan Safire II). l-AuBP1 (WAGAKRLVLRRE) contains a tryptophan (W) residue which is expected to contribute to optical absorbance near 280nm with an extinction coefficient of 5500 M^{-1} cm^{-1} at 280nm (Gasteiger et al., 2005).

Experimental Design

Experimental design and methodology used a semi-iterative approach to explore expected signal responses and used a factorial design of experiments. Many preliminary studies explored synthesis of gold nanoparticles using trisodium citrate as a reducing agent (supplementary information). An initial exploratory round aimed to evaluate precipitation activity of l-AuBP1 and l-AgBP1 in the presence of $HAuCl_4$ and $AgNO_3$ precursors while decreasing the concentration of peptide to precursor ions. Review of this initial exploratory round revealed several sources of error that informed process improvements in the present study (supplementary information). This study was conducted in triplicate, implemented acetate buffer for pH control, and improved measurement fidelity.

		Uncontrolled pH (DI Water)	Controlled pH 3.8 (100mM Acetate)	Controlled pH 5.4 (100mM Acetate)
AuBP1	Au	AuBP1 + HAuCl4	AuBP1 + HAuCl4	AuBP1 + HAuCl4
AuBP1	Ag	AuBP1 + AgNO3	AuBP1 + AgNO3	AuBP1 + AgNO3
AgBP1	Au	AgBP1 + HAuCl4	AgBP1 + HAuCl4	AgBP1 + HAuCl4
AgBP1	Ag	AgBP1 + AgNO3	AgBP1 + AgNO3	AgBP1 + AgNO3
Diluent	AuBP1	AuBP1 + DI Water	AuBP1 + Buffer	AuBP1 + Buffer
Diluent	AgBP1	AgBP1 + DI Water	AgBP1 + Buffer	AgBP1 + Buffer
Diluent	Au	HAuCl4 + DI Water	HAuCl4 + Buffer	HAuCl4 + Buffer
Diluent	Ag	AgNO3 + DI Water	AgNO3 + Buffer	AgNO3 + Buffer

Figure 1 Primary experimental matrix. All combinations are at 1:1 ratio with concentrations of 0.5mM

The main experimental run tested three factors: peptide, precursor, and pH in a full factorial design (figure 1). Two levels of peptide conditions were evaluated (l-AuBP1 and l-AgBP1), two levels of metallic precursors were evaluated ($HAuCl_4$ and $AgNO_3$), and three pH conditions were evaluated (Uncontrolled, pH 3.8, and pH 5.4). A 100mM acetate buffer was used to stabilize pH values in a desired range. Concentration of peptide and precursor ions was fixed at 0.5mM for all conditions. A full factorial design results in 12 treatment combinations with an additional 12 combinations added for isolating background signals and ensuring absence of buffer side reactions.

Prior experience indicated an absence of reaction in those conditions without peptide and precursor. Thus, sampling of optical absorbance was prioritized for conditions containing both peptide and precursors. The UV-Vis spectra of peptide and precursor reactions was sampled in 50 30min intervals, while the spectra of conditions containing only peptide or precursor ions in their respective diluent was measured once following initial sample preparation and once approximately 26 hours thereafter. pH measurement for each condition in each triplicate run was carried out to confirm the effect of the buffer agent.

Results

This section will present the results of the primary experimental matrix in addition to further analysis and characterization. UV-Vis results for reactions of both peptides, l-AuBP1 and l-AgBP1, in both $HAuCl_4$ and $AgNO_3$ precursors are plotted to identify precipitates forming in solution. pH readings for all reaction conditions measure the effectiveness of the buffer control for each of the pH conditions. Scanning electron microscopy (SEM) results illustrate the morphology of particles formed in the reaction of l-AuBP1 with $HAuCl_4$. Mass spectrometry analysis of l-AuBP1 before and following the reaction with $HAuCl_4$ characterizes the formation of new chemical species.

l-AuBP1

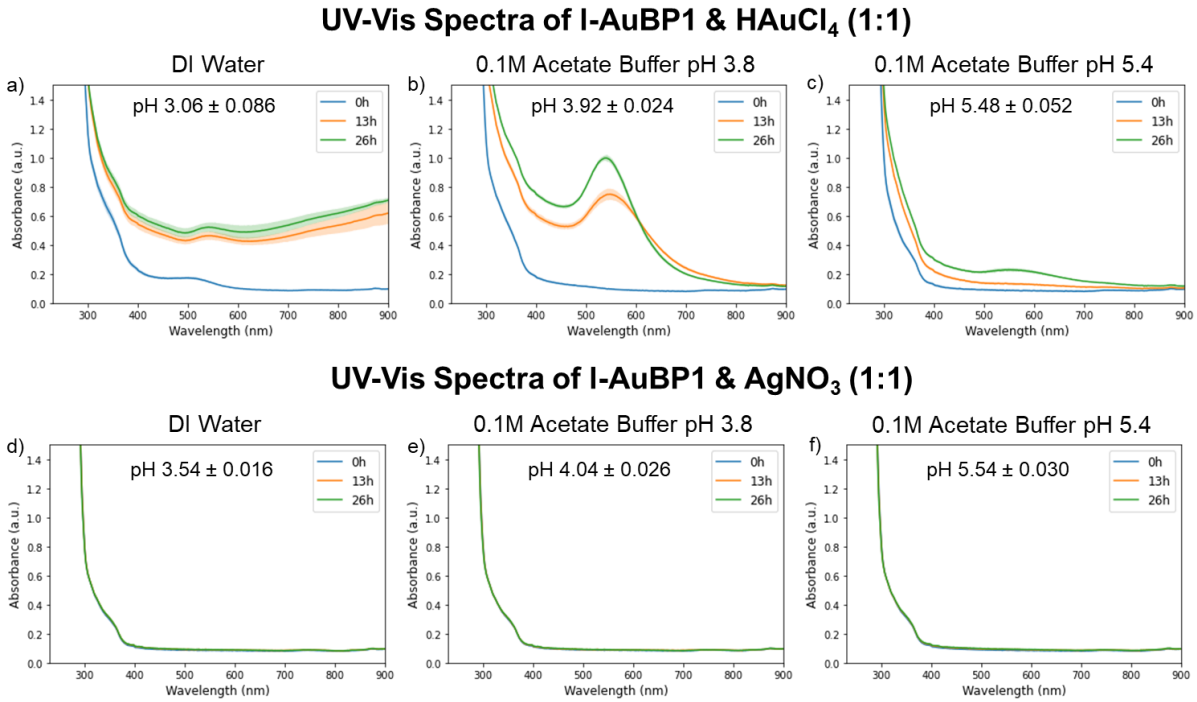

Figure 2 UV-Vis Spectra of l-AuBP1 with $HAuCl_4$ and $AgNO_3$ under different pH conditions

UV-Vis spectra of wells containing l-AuBP1 and $HAuCl_4$ at an equimolar ratio of 0.5mM:0.5mM indicated the formation of nanosized Au (AuNP) precipitates with peaks forming near the region of interest for gold nanoparticles (560 ± 50nm). Three distinct spectra were observed for each of the pH conditions (figure 2 a,

b, c). In DI water, a broad increase in absorption spectra was observed between 300nm and 900nm with a small peak at 546nm. In contrast, samples containing acetate buffer showed more localized increases in absorbance during the reaction. The pH 3.8 condition generated a clear signature of AuNP in solution with a large peak forming at 540nm. The pH 5.4 condition resulted in little increase in optical absorbance compared to both the uncontrolled DI water condition and pH 3.8 condition with a small peak at 548nm. Follow up measurements of UV-Vis spectra after 48 hours indicate the uncontrolled pH and pH 3.8 conditions had reached a stable absorption spectrum after 26h and further increases to absorption were observed for the pH 5.4 condition (supplementary information). The shaded regions of the plots indicating 95% confidence interval shows the uncontrolled pH condition resulted in more variation across the three trials compared to buffered conditions. The UV-Vis spectra of l-AuBP1 and $AgNO_3$ (figure 2 d, e, f) did not show any significant changes within the region of interest for silver nanoparticles (420 ± 50nm) for all pH conditions.

The measured pH of l-AuBP1 and $HAuCl_4$ is approximately 0.48 lower than that of l-AuBP1 and $AgNO_3$ in the DI water condition. Surprisingly the pH variation between DI water trials was the highest for the $HAuCl_4$ condition and the lowest for the $AgNO_3$ condition as indicated by the confidence intervals ± 0.086 and ± 0.016 respectively. In all the $AgNO_3$ conditions the pH tended to be higher that of the $HAuCl_4$ condition for each of the pH levels tested.

		Uncontrolled pH (DI Water)	Controlled pH 3.8 (100mM Acetate)	Controlled pH 5.4 (100mM Acetate)
l-AuBP1 (0.05mM)	Au	AuBP1 + HAuCl4	AuBP1 + HAuCl4	AuBP1 + HAuCl4
l-AuBP1 (0.005mM)	Au	AuBP1 + HAuCl4	AuBP1 + HAuCl4	AuBP1 + HAuCl4

Figure 3 Experimental matrix for a follow up study of l-AuBP1 and $HAuCl_4$ at different concentrations of l-AuBP1

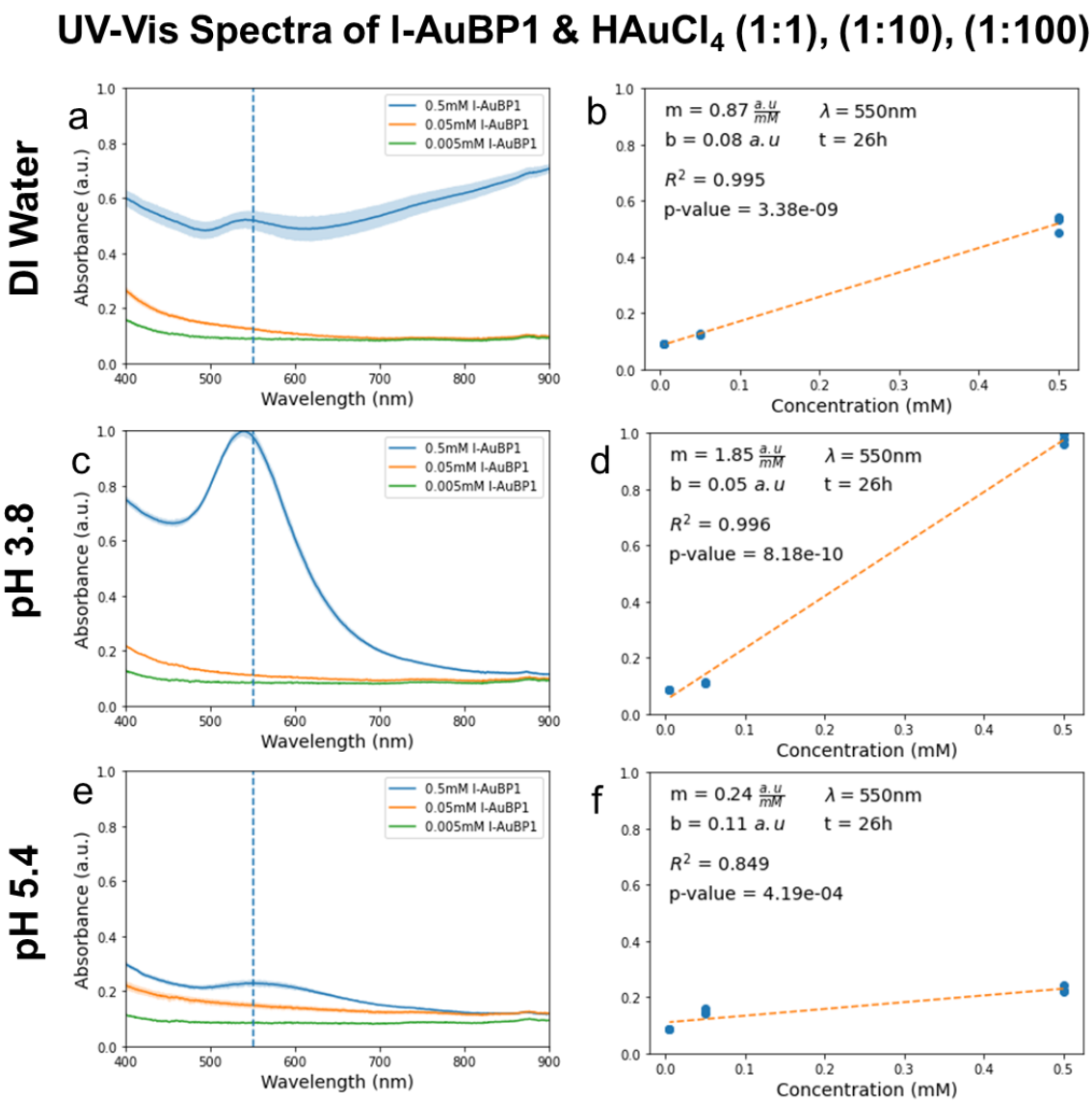

Figure 4 UV-Vis Spectra of l-AuBP1 and $HAuCl_4$ at decreasing concentration of l-AuBP1. Linear relationships are plotted adjacent to their respective UV-Vis plot

A follow up study of l-AuBP1 and $HAuCl_4$ reactions investigating changes to peptide concentration relative to $HAuCl_4$ was carried out to elucidate reaction behavior as a function of available peptide. Triplicate reactions of 0.05mM (1:10) and 0.005mM (1:100) l-AuBP1 with 0.5mM $HAuCl_4$ were carried out on a single plate in the same three pH conditions as the primary experimental matrix (figure 3). These data were combined with the 1:1 condition from the primary run to create the plots above. UV-Vis plots of low l-AuBP1 concentrations after 26 hours of reaction show little increase in absorbance both inside and outside

the regions of interest (figure 4). Absorbance values taken at 550nm after 26h were plotted against peptide concentration to elucidate trends in the absorbance as a function of peptide concentration. The absorbance at this wavelength serves as a heuristic for gold precipitated by the peptide, however many factors including aggregation, particle size, and particle shape contribute to overall absorbance profile.

Plots b, d, and f of figure 4 include a linear regression of the absorbance values with nine data points in total (three absorbance values for each triplicate). Concentration values were assigned as prepared from stock solution and do not represent measured values. The slope of the line represents optical absorbance at 550nm after 26 hours as a function of peptide concentration. Comparison of the slope values for each of the plots reveals that the pH 3.8 condition yields the highest (1.85) followed by the DI water condition (0.87) and the pH 5.4 condition (0.24). The DI water and pH 3.8 conditions show a linear response with R squared values of 0.995 and 0.996 respectively while the pH 5.4 condition has an R squared value of 0.849. Low p-values for each of the linear plots indicate results were replicated consistently across trials.

l-AgBP1

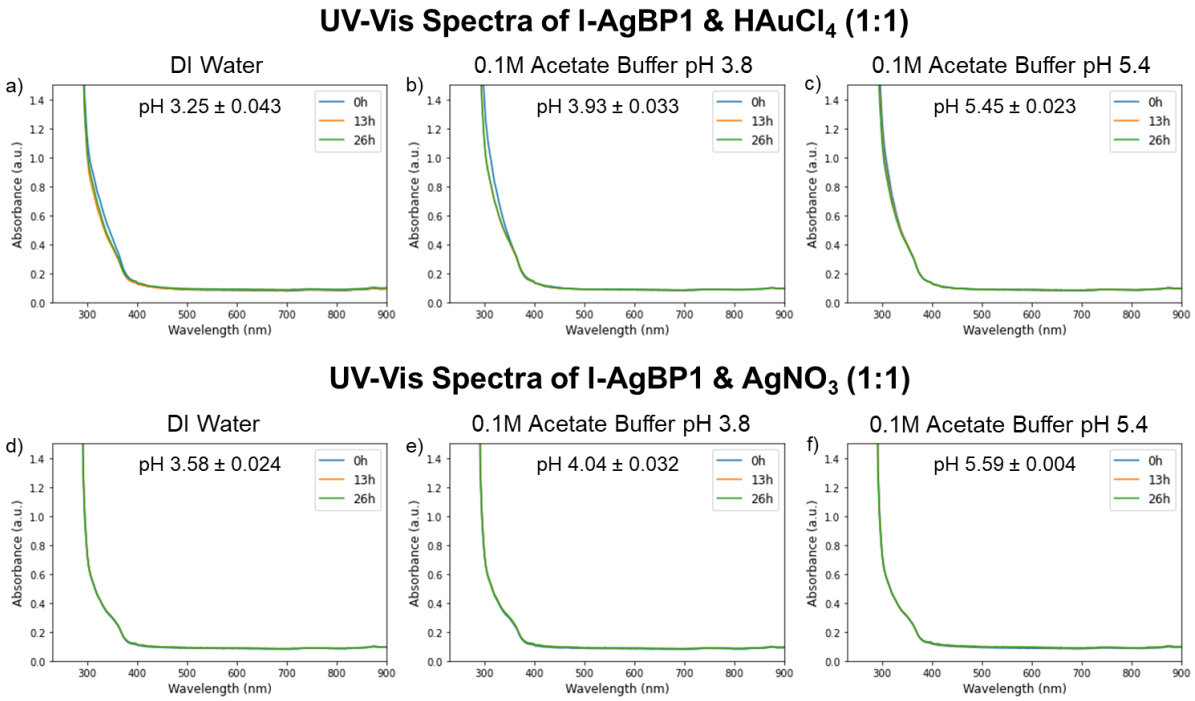

Figure 5 UV-Vis Spectra of l-AgBP1 with $HAuCl_4$ and $AgNO_3$ under different pH conditions

UV-Vis spectra from wells containing l-AgBP1 showed remarkably little activity for both $HAuCl_4$ and $AgNO_3$ (figure 5). Slight decreases in absorbance between 300 – 400nm were observed for wells containing l-AgBP1 and $HAuCl_4$. Follow up measurements conducted after 48 hours reveals slight increases to optical absorbance for the pH 5.4 condition in wells containing $AgNO_3$ (supplementary information). pH measurements for the wells containing $AgNO_3$ were generally higher than wells containing $HAuCl_4$ consistent with prior observations with l-AuBP1 containing wells. As observed in the l-AuBP1 conditions, pH of the wells containing $AgNO_3$ was slightly higher than for wells containing $HAuCl_4$.

pH Measurements

pH color scale: 3.0 – 6.0

(0.5mM)	(0.5mM)	Uncontrolled pH (DI water) Mean	±	Controlled pH 3.8 (100mM Acetate) Mean	±	Controlled pH 5.4 (100mM Acetate) Mean	±
l-AuBP1	Au	3.06	0.086	3.92	0.024	5.48	0.052
l-AuBP1	Ag	3.54	0.016	4.04	0.026	5.54	0.030
l-AgBP1	Au	3.25	0.043	3.93	0.033	5.45	0.023
l-AgBP1	Ag	3.58	0.024	4.04	0.032	5.59	0.004
Diluent	l-AuBP1	3.52	0.094	4.05	0.038	5.59	0.051
Diluent	l-AgBP1	3.71	0.095	4.05	0.039	5.61	0.043
Diluent	Au	3.61	0.042	3.97	0.031	5.52	0.030
Diluent	Ag	3.87	0.106	4.06	0.054	5.62	0.015
l-AuBP1 (0.05mM)	Au	3.43	0.034	3.99	0.014	5.46	0.058
l-AuBP1 (0.005mM)	Au	3.56	0.014	4.00	0.007	5.45	0.019
Diluent Controls*		3.87	0.107	4.08	0.002	5.62	0.033

*Duplicate readings

Figure 6 pH measurements (red to green) for reaction condition with a 95% confidence interval (red to white)

Measurements of pH were carried out in triplicate following UV-Vis measurements of the primary experimental matrix and the follow up study with l-AuBP1. Figure 6 reports the average pH for each of the triplicates (red to green coloring) along with a 95% confidence interval (red to white coloring). As expected, the wells containing DI water as the primary diluent showed the highest degree of variability while the buffered solutions showed lower variability as indicated by narrower confidence intervals. The pH 3.8 condition turns out to be closer to a pH of 4.01 ± 0.035 while the pH 5.4 condition turns out to be close to 5.55 ± 0.031 when averaging across each well per pH condition.

SEM

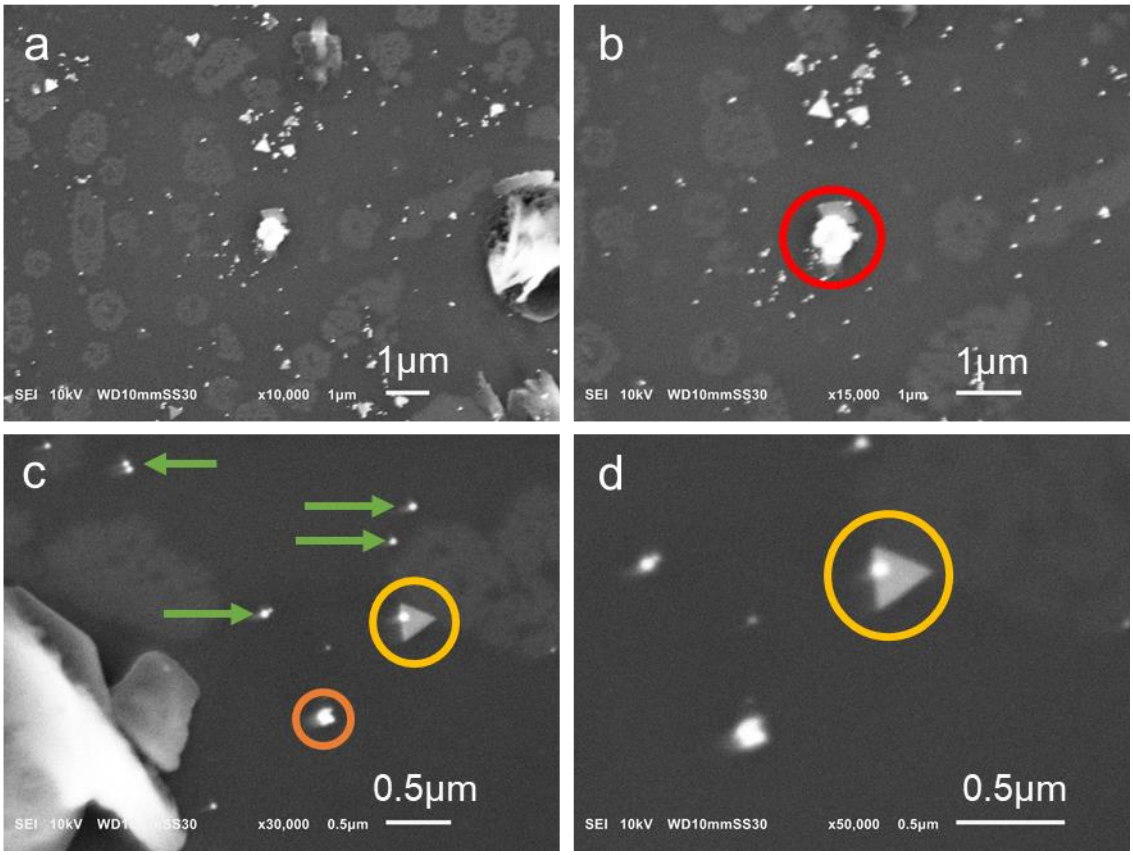

Figure 7 SEM Micrographs of particles formed by l-AuBP1 and $HAuCl_4$

SEM images were taken for one sample reaction of l-AuBP1 and $HAuCl_4$ with several features highlighted. Individual AuNP particles approximately 50nm in size are pointed out by the green arrows in figure 7 (c). Large and small agglomerations of AuNPs are circled in red and orange (figure 7 b and c). Particles with equilateral triangular morphology with side lengths of approximately 300nm are among the morphological species observed circled in subplot (figure 7 c and d). Presence of triangular shape preserving growth morphologies suggests growth inhibition of specific crystallographic directions. Preferential binding of l-AuBP1 to a specific facet could explain the occurrence of this relatively large morphological species.

Mass Spectrometry

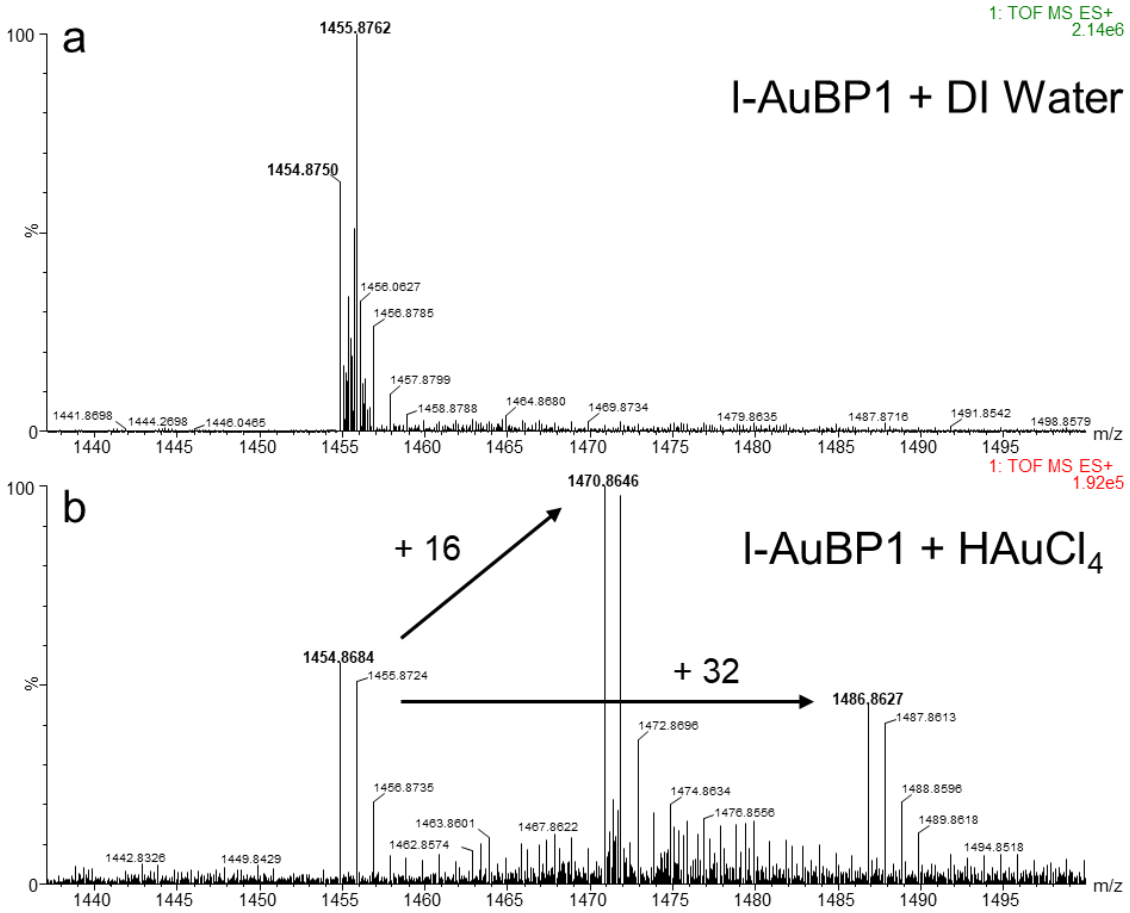

Figure 8 Mass spectrometry results of l-AuBP1 in DI water (a) and l-AuBP1 reacted with $HAuCl_4$ (b).

Mass spectrometry was carried out to investigate possible changes in solution chemistry due to reaction of l-AuBP1 and $HAuCl_4$. The top spectral window represents molecular species from l-AuBP1 dissolved in DI water (figure 8 a) and the bottom spectral window represents molecular species from the l-AuBP1 and $HAuCl_4$ reaction conducted in DI water (figure 8 b). The DI water condition was chosen because the pH-controlled reactions contain relatively high salt concentrations which can introduce noise in liquid chromatography mass spectrometry analysis. Comparison of the two selected spectral windows indicates the formation of two high molecular weight adducts as a result of the reaction with masses of (1470.86) and (1486.86). Small shifts off the defined masses represent their isotropic envelopes.

Discussion

The motivation behind these experiments is to characterize differences in precipitation between two metal binding peptides l-AuBP1 and l-AgBP1 in the metallic precursors of the solids for which they were originally selected. Investigating selectivity of the two peptides and mechanism of precipitation is essential for evaluating potential use in concentration and separation processes in hydrometallurgy. This section aims to discuss the results and their implications and identify sources of error.

A broad comparison of the UV-Vis results between l-AuBP1 and l-AgBP1 show differences and similarities in metal precipitation activity. For solutions with $HAuCl_4$ precursor, only l-AuBP1 demonstrates precipitation activity while l-AgBP1 shows no indication of $HAuCl_4$ precipitation under the tested conditions. Both l-AuBP1 and l-AgBP1 do not show any precipitation activity for $AgNO_3$ in DI water or acetate buffered solutions.

Characteristics of the selected precursor solutions offer a possible explanation of the observed precipitation behavior. Because Ag(I) has a lower charge than Au(III), $AgNO_3$ more readily dissociates into Ag^+ and NO_3^- than $HAuCl_4$ where pH plays a significant role in ionic speciation. At pH < 6.0, planar $AuCl_4^-$ ions are the dominant species with OH^- ligand substitutions for Cl^- occurring at pH > 6.0 (Peck et al., 1991). pH measurements of reactions in this study all fall below 6.0 indicating the dominant species in solution is $AuCl_4^-$. However, l-AuBP1 mediated gold precipitation drops off significantly at the high pH condition (5.48 ± 0.052). A change in precursor speciation could influence standard reduction potentials and peptide-ion interactions resulting in less precipitation activity and thus attenuated UV-Vis absorbance spectra.

Table 1 Redox half reaction potentials for $HAuCl_4$ and $AgNO_3$

	Redox half reaction	E° (V)*
$HAuCl_4$	$AuCl_4^- + 3e^- \rightleftharpoons Au_{(s)} + 4Cl^-$	1.002
$AgNO_3$	$Ag^+ + e^- \rightleftharpoons Ag_{(s)}$	0.7996

*P1: Standard Reduction Potentials by Element. (2013)

A distinct lack of Ag reduction in this study may be explained by several factors. Comparison of the standard reduction potential for the two ionic precursor species shows that $AuCl_4^-$ is approximately 0.2V higher that than of Ag^+ (table 1). The higher reduction potential of $AuCl_4^-$ indicates

easier acceptance of electrons than Ag^+ meaning $AuCl_4^-$ is more likely to reduce to $Au_{(s)}$ than Ag^+ is to reduce to $Ag_{(s)}$. The redox potential of the solution measures its capacity for facilitating electron transfer and the standard reference reduction potential (E_h) is directly related to pH through the Nernst equation. Low pH favors an oxidizing environment while a high pH favors a reducing environment. A study of aqueous synthesis of Ag nanoparticles by Pris in 2014 using common reducing agents found that 1:1 concentrations of sodium citrate to $AgNO_3$ resulted in extremely slow reaction kinetics at room temperature and formation of aggregates. Their result found optimal synthesis of stabilized silver nanoparticles at 70°C, pH 10, and concentration ratio of 5:1 sodium citrate to $AgNO_3$. The relatively low pH and temperature in this study were clearly not conducive for Ag^+ reduction by neither peptide nor sodium citrate (supplementary information) in the time scale considered in this study.

Table 2 Comparison of l-AuBP1 and l-AgBP1 sequence characteristics

Name	Sequence (12 AA)	Charge	MW:	Theoretical pI	GRAVY
l-AuBP1	W A G A K R L V L R R E	3+	1454.74	11.71	-0.567
l-AgBP1	T G I F K S A R A M R N	3+	1351.59	12.01	-0.458

web.expasy.org/protparam (Gasteiger et al., 2005)

Amino Acid Side Chain Chemistry Legend

Aromatic [F,W,Y]	Acidic (-) [D,E]	Basic (+) [R, H, K]	Nonpolar (Aliphatic) [A, G, I, L, M, P, V]	Polar (neutral) [C, N, Q, S, T]

The differences in $HAuCl_4$ precipitation by l-AuBP1 and l-AgBP1 are explained by unique chemistry and conformation resulting from amino acid composition and sequence (table 2). Despite relatively low sequence similarity (60% identity over 5 residues) both peptides, l-AuBP1 and l-AgBP1, have the same charge, similar theoretical isoelectric points (pI), and similar hydropathy (GRAVY). However, differences between these peptides are of interest for explaining their corresponding precipitation activity. Aromatic ring-containing amino acids tryptophan (W) and phenylalanine (F) present likely sites of oxidation and are found in l-AuBP1 and l-AgBP1 respectively. The indole ring present in tryptophan is more electron rich and as a result more easily oxidizable compared to the benzene ring found in phenylalanine. Additionally, the tryptophan residue located at the N terminus of l-AuBP1 allows for more unshielded interactions with the surrounding solution than the phenylalanine present at the fourth position in l-AgBP1. Comparison of

the vertical ionization energy of phenylalanine (8.7 eV) with tryptophan (7.3 eV) indicates less energy is needed to remove an electron from tryptophan than phenylalanine (Roy et al. 2018). The lack of $HAuCl_4$ reduction by l-AgBP1 could be due to higher energy barriers for electron donation and lower solution interaction due to surrounding residues compared to l-AuBP1. The clear reduction of $HAuCl_4$ by l-AuBP1 is likely due to the more permissible and easily oxidizable tryptophan residue at the N terminus.

A peptide acting as a catalyst for metallic precipitation could prove valuable in hydrometallurgical contexts allowing functional peptide agents to be potentially reused for multiple rounds of metallic concentration and separation. A follow up study investigating how lower ratios of l-AuBP1 to $HAuCl_4$ influenced its reduction was carried out to see whether l-AuBP1 was consumed in the reduction of $HAuCl_4$. If l-AuBP1 is consumed in the reduction process, then greatly attenuated UV-Vis absorbance would be expected commensurate with the decrease in concentration. The results collected in the follow up study in figure 4 show a direct relationship of decreasing UV-Vis absorbance (after 26 hours) with decreases in l-AuBP1 concentration in an approximately linear fashion for each of the pH conditions. This trend indicates that l-AuBP1 likely acts as a limiting reactant and is consumed in the reduction of $HAuCl_4$. Consumption of l-AuBP1 in the reduction of $HAuCl_4$ indicates a likely oxidative chemical modification to l-AuBP1 following the apparent redox reaction.

Table 3 Comparison of experimental mass with theoretical mass for l-AuBP1 and adducts

	C	H	N	O	Calc. Mass	Mass	PPM
l-AuBP1	65	112	23	15	1454.8708	1454.8684	-1.6
l-AuBP1-O	65	112	23	16	1470.8657	1470.8646	-0.7
l-AuBP1-OO	65	112	23	17	1486.8607	1486.8627	1.3

Mass spectrometry analysis carried out on l-AuBP1 (figure 8) shows oxidative damage done to l-AuBP1 while reducing $Au^{3+}_{(aq)}$ to $Au^{0}_{(s)}$. Two prominent adducts of l-AuBP1 with molecular weights of (1470.86) and (1486.86) likely correspond to the addition of one and two oxygen atoms (15.999amu) respectively. Comparison of experimentally observed mass with theoretical mass for one and two oxygen additions to l-AuBP1 shows exceptional agreement with less than 2ppm error (table 3). Tryptophan (W or Trp) present

in l-AuBP1 (WAGAKRLVLRRE) is strongly implicated in the reduction of $HAuCl_4$ (Ozaki et al, 2020). A search for Trp degradation products reveals that its indole group is highly susceptible to oxidation and Trp is involved in several metabolic pathways in the production of serotonin, melatonin, and kynurenine (Bellmaine et al., 2020).

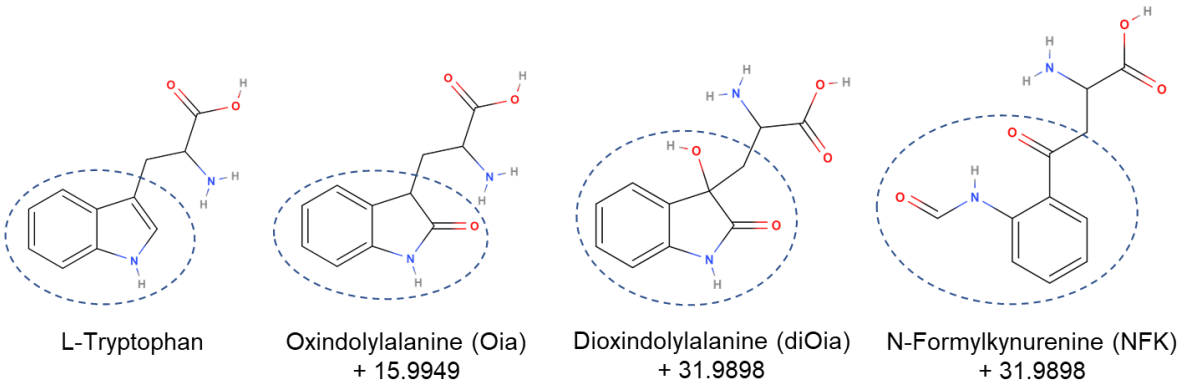

Figure 9 Unmodified L-Tryptophan and possible degradation products of Tryptophan residues in a peptide.

Out of the direct oxidation products of Trp in proteins and peptides described by Bellmaine et al., 2020, three possible residue species correspond with observed increases in mass in this study (figure 9). Oxindolylalanine (Oia) corresponds to the addition of a single oxygen to the indole ring of Trp. Transformation of the Trp residue in l-AuBP1 to Oia would explain the newly observed molecular species with a mass of 1470.86 (1454.86 + 15.9949) following a redox reaction with $HAuCl_4$. Both Dioxindolylalanine (diOia) and N-Formylkynurenine (NFK) correspond to the addition of two oxygen atoms to Trp. DiOia adds an oxygen and hydroxyl group (OH) to the indole ring while NFK results in a cleavage of the indole ring and the addition of two double bonded oxygen atoms. Transformation of Trp into either a diOia or NFK residue within l-AuBP1 would explain the newly observed molecular species with a mass of 1486.86 (1454.86 + 31.9898). However, it is difficult to determine the dominant +32amu species with the collected data. Further exploration of NFK formation seems to indicate a possible intermediate corresponding to a single oxygen addition during the synthesis of NFK from free Trp (not a part of a protein or peptide) (Basran et al., 2011). The chemical alteration of the Trp residue is not easily

reversible and likely indicates a loss of functionality similar to protein oxidation in the body (Cecarini et al. 2007).

The term biomineralization conjures up a wide range of biomolecular interactions with inorganics focused on the transformation of aqueous precursors into solid species. However, there are several modalities by which peptide mediated biomineralization or precipitation can occur. The one in this study is the reduction of a metallic precursor into solid elemental form through the oxidation of a residue on the peptide like the mechanism described in Tomizaki et al. (2020). Another as described by Hatanaka et al. (2017) and Dai et al. (2005) operates through a surface stabilization regime interacting with multiple ions to form an insoluble species. While strong surface binding certainly plays a role in surface stabilization, de novo designed peptides described in Tomizaki et al. (2020) accomplish reduction of $HAuCl_4$ primarily through electron donation without the need for stabilizing multiple ionic species through surface interaction.

How could peptide guided selective precipitation improve sustainability in separation and concentration processes in hydrometallurgy? Alteration of inorganic species stability in aqueous solutions could be used to reduce use of caustic reagents and potentially decrease temperatures required for certain reactions. A higher degree of molecular specificity and selectivity could allow for a more targeted approach in metals separation resulting in potentially fewer processing steps. Use of natural peptides and proteins could allow for biogenic production making use of organic waste streams. Because l-AuBP1 is oxidized in the process of reducing $HAuCl_4$, its potential for improving the sustainability of hydrometallurgy processes is limited because it would require constant regeneration with new unoxidized peptides. In contrast, a biosorption approach allows a single functional agent to be reused multiple times without the need for maintaining cell viability (Mattocks & Cotruvo, 2020). For a biomineralizing peptide to be used multiple times in a hydrometallurgy process, a reversible surface stabilization regime or regenerative redox reaction would be required.

Review of the experimental protocols was conducted to identify potential sources of error. Manual pipetting implemented in the reagent preparation could introduce small variations in stock concentrations.

Fluctuations in room temperature can change the pH and free energy of the solutions. Temperature plots for each of the trials can be found in the supplementary information. Each trial in the triplicate was prepared using the same stock of reagents and an error in the initial stage could have been replicated across each trial. Measurement and transfer of 3-5mg of lyophilized dry peptide was tricky because static electricity caused small chunks to move erratically. This was partially mitigated by using aluminum foil in place of weighing paper. Measurement of pH was done with two different probes, one for the initial preparation of the reagents and another for the follow up measurements in the well. The pH measurements in the well were carried out in small volumes (250µL) and took between two and ten minutes to stabilize. Determining if the pH reading had fully stabilized was sometimes difficult due to the long stabilization times. The plate was fully uncovered during pH measurements which took around two hours for each trial which likely led to some evaporation and changes in concentration. These changes in concentration may have impacted the pH readings.

Conclusions & Future Work

Controlling morphology of nanomaterials is the primary focus of literature concerning peptide guided nanoparticle synthesis while biosorption is the primary focus of functional peptides and proteins in hydrometallurgy. Probing their intersection yields relevant results valuable for many applications. Within this study we find that l-AuBP1 reduces $HAuCl_4$ in both DI water and acetate buffered solutions with diminished reduction activity near pH 5.4. We find that l-AgBP1 forms neither Au or Ag nanoparticles at room temperature and acidic pH. Comparing different mechanisms of peptide guided precipitation illustrated two distinct regimes 1) surface stabilization of a compound and 2) metallic reduction through a redox reaction. Further investigation of l-AuBP1 confirms a drop off in $HAuCl_4$ reduction as peptide concentration decreases and clear oxidation of l-AuBP1 following reduction of $HAuCl_4$. These two factors show the limitations of l-AuBP1 in hydrometallurgy and help illustrate useful characteristics like reusability to guide the focus of future studies.

The future work described here has two aims 1) to strengthen the claims and results of the present study and 2) to suggest alternative avenues of research. For the former, improvements to protocol design should implement strict temperature control and each trial should be conducted in an isolated approach to prevent propagation of errors in the stock preparation stage. Larger reaction vessels should be implemented to minimize effects of evaporation and improve reliability of pH measurements. UV-Vis measurements should be readjusted to focus on longer time scales for reactions with slow kinetics. Larger amounts of peptide should be used to prepare more accurate stock reagents. To strengthen the claims of the present study: Mass spec should be carried out for each of the reactions of peptide and metallic precursor. Better positive controls should be developed for identifying the formation of gold and silver nanoparticles using common reducing agents like sodium citrate, ascorbic acid, and sodium borohydride. Multiple negative control peptides with sequence similarities to l-AuBP1 and l-AgBP1 should be used to compare functional characteristics. Mutations of l-AuBP1 and l-AgBP1 should be evaluated to identify the role of key residues. Potential mutants of l-AuBP1 and l-AgBP1 would include an alanine scan, substitution of different natural aromatic residues, and placing aromatic residues at different locations. Evaluating circular forms of l-AuBP1 and l-AgBP1 to study the role of conformation could yield insights for design improvements. TEM instead of SEM imaging should be carried out for improved resolution and a more systematic review of solution precipitates may inform aspects of nucleation and growth at different points in the reaction.

In a broader perspective, future work in this area should examine more realistic processing conditions where peptide guided selective precipitation could replace an existing toxic and energy intensive process. For the potential of selective peptide guided precipitation to be realized there needs to be a stronger focus on molecular reusability and platforms for biogenic production. Any potential candidates for process improvement should undergo full LCA analysis to back up claims of sustainability.

Materials & Methods

Peptide Synthesis: l-AuBP1 (MW:1454.72) and l-AgBP1 (MW: 1351.57) were synthesized by BIOMATIK at >95% purity with no terminal modifications (free amine and free acid) and no TFA removal. Purity and molecular weight were confirmed by HPLC and Mass Spectroscopy.

Mineralization: Chloroauric acid $HAuCl_4$ (Sigma Aldrich HT1004-100ML) and Silver Nitrate Solution $AgNO_3$ (Innovating Science: 0724832004875) were used as metallic precursors diluted with either DI water or 0.1M acetate buffer solution. Precursor solutions were combined in equal volumes of 125μL for a final reaction volume of 250μL in a standard flat bottom 96 well plate.

UV-Vis Spectroscopy: A Tecan Safire II was used for measuring the UV-Vis response of mineralization reactions. Optical absorbance was collected from 230nm-900nm in kinetic intervals of 30min and 60min. The plots were created by averaging absorbance spectra across three trials and calculating a 95% confidence interval on a per wavelength basis to generate the shaded regions. Three time points at 0, 13, and 26 hours are plotted for clarity.

SEM Imaging: A small aliquot was taken from one l-AuBP1 and $HAuCl_4$ reaction and diluted with isopropyl alcohol and spotted onto a silicon wafer. The wafer with the particles on the surface was placed in a desiccator to fully dry prior to imaging. Imaging was carried out on a JEOL JSM-6010 Plus.

pH Measurements: A spear tip pH probe (Atlas Scientific ENV-45-pH) allowed full contact of the probe tip in wells containing 250uL of solution. Stabilization of pH readings during measurement often required several minutes. pH readings were recorded over serial interface with readouts every 2s and allowed to stabilize for at least 5 minutes with some wells requiring more or less time to stabilize. Final readings were calculated by averaging the last 10 pH read outs from the serial interface before washing with DI water.

Mass Spectrometry: Sample analysis was carried out at UW-Medicinal Chemistry Mass Spectrometry Center using a Waters G2-XS TOF. Sample was injected as delivered. A gradient on a Waters 2.1x100 CSH column using 0.1% FA in H2O & 0.1% FA in ACN as mobile phase.

Molecular Illustration: Possible tryptophan degradation products were modelled using the online tool at molview.org

Acknowledgements

I would first like to thank Prof. Lucien Brush for supervising this project and Prof. Joyce Cooper for participating in my masters committee. I also would not have begun this project and been prepared to tackle this work without the initial support of Prof. Mehmet Sarikaya and the facilities of the GEMSEC lab.

My sincere thanks goes out to Dr. Hanson Fong who supported my experimental work and helped tackle many issues in the lab and Dr. Deniz Yucesoy provided valuable insights on peptide characteristics. I would also like to thank Siddharth Rath for stimulating conversations and Zoey Surma for answering my many chemistry related questions. Further, I could not have done this without the foundational work carried out by Marketa Hnilova (PhD) and former graduate students of the GEMSEC lab.

Dale Whittington, unsung hero of the UW - Medicinal Chemistry Mass Spectrometry Center provided valuable and expeditious mass spec analysis.

Masters project funding and lab facilities provided by the UW Materials Science and Engineering department allowed me to carry out this fulfilling work and I greatly appreciate the administrative faculty for helping me navigate obstacles.

References

Bellmaine, Stephanie, Alisa Schnellbaecher, and Aline Zimmer. “Reactivity and Degradation Products of Tryptophan in Solution and Proteins.” Free Radical Biology and Medicine 160 (November 2020): 696–718. https://doi.org/10.1016/j.freeradbiomed.2020.09.002.

Cecarini, Valentina, Jillian Gee, Evandro Fioretti, Manila Amici, Mauro Angeletti, Anna Maria Eleuteri, and Jeffrey N. Keller. “Protein Oxidation and Cellular Homeostasis: Emphasis on Metabolism.” Biochimica et Biophysica Acta (BBA) - Molecular Cell Research 1773, no. 2 (February 1, 2007): 93–104. https://doi.org/10.1016/j.bbamcr.2006.08.039.

Chandra, Kavita, Vished Kumar, Stephanie E. Werner, and Teri W. Odom. “Separation of Stabilized MOPS Gold Nanostars by Density Gradient Centrifugation.” ACS Omega 2, no. 8 (August 31, 2017): 4878–84. https://doi.org/10.1021/acsomega.7b00871.

Chen, Rong, Jiliang Wu, Hui Li, Gang Cheng, Zhong Lu, and Chi-Ming Che. “Fabrication of Gold Nanoparticles with Different Morphologies in HEPES Buffer.” Rare Metals 29, no. 2 (April 1, 2010): 180–86. https://doi.org/10.1007/s12598-010-0031-5.

Chen, Feng, Yanwei Wang, Jun Ma, and Guangcan Yang. “A Biocompatible Synthesis of Gold Nanoparticles by Tris(Hydroxymethyl)Aminomethane.” Nanoscale Research Letters 9, no. 1 (May 7, 2014): 220. https://doi.org/10.1186/1556-276X-9-220.

Choe, W.-S., Sastry, M. S. R., Thai, C. K., Dai, H., Schwartz, D. T., & Baneyx, F. (2007). Conformational Control of Inorganic Adhesion in a Designer Protein Engineered for Cuprous Oxide Binding. Langmuir, 23(23), 11347–11350. https://doi.org/10.1021/la702414m

Dickerson, M. B., Sandhage, K. H., & Naik, R. R. (2008). Protein- and Peptide-Directed Syntheses of Inorganic Materials. Chemical Reviews, 108(11), 4935–4978. https://doi.org/10.1021/cr8002328

Dogan, S., Fong, H., Yucesoy, D. T., Cousin, T., Gresswell, C., Dag, S., Huang, G., & Sarikaya, M. (2018). Biomimetic Tooth Repair: Amelogenin-Derived Peptide Enables in Vitro Remineralization of Human Enamel. ACS Biomaterials Science & Engineering, 4(5), 1788–1796. https://doi.org/10.1021/acsbiomaterials.7b00959

Donatan, S., Yazici, H., Bermek, H., Sarikaya, M., Tamerler, C., & Urgen, M. (2009). Physical elution in phage display selection of inorganic-binding peptides. Materials Science and Engineering: C, 29(1), 14–19. https://doi.org/10.1016/j.msec.2008.05.003

Fang, Y., Poulsen, N., Dickerson, M. B., Cai, Y., Jones, S. E., Naik, R. R., Kroger, N., & Sandhage, K. H. (2008). Identification of peptides capable of inducing the formation of titania but not silica via a subtractive bacteriophage display approach. Journal of Materials Chemistry, 18, 3871–3875.

Free, M. L. (2013). Hydrometallurgy: Fundamentals and Applications. John Wiley & Sons.

Gasteiger E., Hoogland C., Gattiker A., Duvaud S., Wilkins M.R., Appel R.D., Bairoch A.; Protein Identification and Analysis Tools on the ExPASy Server; (In) John M. Walker (ed): The Proteomics Protocols Handbook, Humana Press (2005). pp. 571-607

Hatanaka, T., Matsugami, A., Nonaka, T., Takagi, H., Hayashi, F., Tani, T., & Ishida, N. (2017). Rationally designed mineralization for selective recovery of the rare earth elements. Nature Communications, 8(1), 15670. https://doi.org/10.1038/ncomms15670

Hnilova, M., Oren, E. E., Seker, U. O. S., Wilson, B. R., Collino, S., Evans, J. S., Tamerler, C., & Sarikaya, M. (2008). Effect of Molecular Conformations on the Adsorption Behavior of Gold-Binding Peptides. Langmuir, 24(21), 12440–12445. https://doi.org/10.1021/la801468c

Hnilova, M., Liu, X., Yuca, E., Jia, C., Wilson, B., Karatas, A. Y., Gresswell, C., Ohuchi, F., Kitamura, K., & Tamerler, C. (2012). Multifunctional Protein-Enabled Patterning on Arrayed Ferroelectric Materials. ACS Applied Materials & Interfaces, 4(4), 1865–1871. https://doi.org/10.1021/am300177t

Johnson, D. B. (2013). Development and application of biotechnologies in the metal mining industry. Environmental Science and Pollution Research, 20(11), 7768–7776. https://doi.org/10.1007/s11356-013-1482-7

Khatayevich, D., Page, T., Gresswell, C., Hayamizu, Y., Grady, W., & Sarikaya, M. (2014). Selective Detection of Target Proteins by Peptide-Enabled Graphene Biosensor. Small, 10(8), 1505–1513. https://doi.org/10.1002/smll.201302188

Knecht, M. R., & Wright, D. W. (2003). Functional analysis of the biomimetic silica precipitating activity of the R5 peptide from Cylindrotheca fusiformis. Chemical Communications, 24, 3038–3039. https://doi.org/10.1039/B309074D

Kröger, N., Dickerson, M. B., Ahmad, G., Cai, Y., Haluska, M. S., Sandhage, K. H., Poulsen, N., & Sheppard, V. C. (2006). Bioenabled Synthesis of Rutile (TiO2) at Ambient Temperature and Neutral pH. Angewandte Chemie International Edition, 45(43), 7239–7243. https://doi.org/10.1002/anie.200601871

Mattocks, J. A., & Cotruvo, J. A. (2020). Biological, biomolecular, and bio-inspired strategies for detection, extraction, and separations of lanthanides and actinides. Chemical Society Reviews, 49(22), 8315–8334. https://doi.org/10.1039/D0CS00653J

Oren, E. E., Tamerler, C., Sahin, D., Hnilova, M., Seker, U. O. S., Sarikaya, M., & Samudrala, R. (2007). A novel knowledge-based approach to design inorganic-binding peptides. Bioinformatics, 23(21), 2816–2822. https://doi.org/10.1093/bioinformatics/btm436

Ozaki, Makoto, Shuhei Yoshida, Maho Oura, Takaaki Tsuruoka, and Kenji Usui. “Effect of Tryptophan Residues on Gold Mineralization by a Gold Reducing Peptide.” RSC Advances 10, no. 66 (2020): 40461–66. https://doi.org/10.1039/D0RA07098J.

P1: Standard Reduction Potentials by Element. (2013, December 2). Chemistry LibreTexts. https://chem.libretexts.org/Ancillary_Materials/Reference/Reference_Tables/Electrochemistry_Tables/P1%3A_Standard_Reduction_Potentials_by_Element

Pris, M. “Influence of Different Parameters on Wet Synthesis of Silver Nanoparticles.” Undefined, 2014. https://www.semanticscholar.org/paper/Influence-of-different-parameters-on-wet-synthesis-Pris/86652b73c17afab38fa700378d3771a189fc1003.

Peck, Julia A., C. Drew Tait, Basil I. Swanson, and Gordon E. Brown. “Speciation of Aqueous Gold(III) Chlorides from Ultraviolet/Visible Absorption and Raman/Resonance Raman

Roy, Anirban, Robert Seidel, Gaurav Kumar, and Stephen E. Bradforth. “Exploring Redox Properties of Aromatic Amino Acids in Water: Contrasting Single Photon vs Resonant Multiphoton Ionization in Aqueous Solutions.” The Journal of Physical Chemistry B 122, no. 14 (April 12, 2018): 3723–33. https://doi.org/10.1021/acs.jpcb.7b11762.

Sarikaya, M., Tamerler, C., Jen, A. K.-Y., Schulten, K., & Baneyx, F. (2003). Molecular biomimetics: Nanotechnology through biology. Nature Materials, 2(9), 577–585. https://doi.org/10.1038/nmat964

Slocik, J. M., Naik, R. R., Stone, M. O., & Wright, D. W. (2005). Viral templates for gold nanoparticle synthesis. Journal of Materials Chemistry, 15(7), 749–753. https://doi.org/10.1039/B413074J

Tamerler, C., Kacar, T., Sahin, D., Fong, H., & Sarikaya, M. (2007). Genetically engineered polypeptides for inorganics: A utility in biological materials science and engineering. Materials Science and Engineering: C, 27(3), 558–564. https://doi.org/10.1016/j.msec.2006.05.046

Thai, C. K., Dai, H., Sastry, M. S. R., Sarikaya, M., Schwartz, D. T., & Baneyx, F. (2004). Identification and characterization of Cu2O- and ZnO-binding polypeptides by Escherichia coli cell surface display: Toward an understanding of metal oxide binding. Biotechnology and Bioengineering, 87(2), 129–137. https://doi.org/10.1002/bit.20149

Tomizaki, Kin-ya, Takuya Okamoto, Tatsuki Tonoda, Takahito Imai, and Masahiro Asano. "Selective Gold Recovery from Homogenous Aqueous Solutions Containing Gold and Platinum Ions by Aromatic Amino Acid-Containing Peptides." International Journal of Molecular Sciences 21, no. 14 (January 2020): 5060. https://doi.org/10.3390/ijms21145060.

Tomizaki, Kin-ya, Shota Wakizaka, Yuichi Yamaguchi, Akitsugu Kobayashi, and Takahito Imai. "Ultrathin Gold Nanoribbons Synthesized within the Interior Cavity of a Self-Assembled Peptide Nanoarchitecture." Langmuir 30, no. 3 (January 28, 2014): 846–56. https://doi.org/10.1021/la4044649.

UV-Vis Spectroscopy Open Source Reference Data Library for Nanoparticles. (2021, April 23). InstaNANO. https://instanano.com/characterization/reference/uv-vis-spectroscopy/

Vahidi, E., & Zhao, F. (2017). Environmental life cycle assessment on the separation of rare earth oxides through solvent extraction. Journal of Environmental Management, 203, 255–263. https://doi.org/10.1016/j.jenvman.2017.07.076

Yazici, H., Fong, H., Wilson, B., Oren, E. E., Amos, F. A., Zhang, H., Evans, J. S., Snead, M. L., Sarikaya, M., & Tamerler, C. (2013). Biological response on a titanium implant-grade surface functionalized with modular peptides. Acta Biomaterialia, 9(2), 5341–5352. https://doi.org/10.1016/j.actbio.2012.11.004

Zin, M. T., Munro, A. M., Gungormus, M., Wong, N.-Y., Ma, H., Tamerler, C., Ginger, D. S., Sarikaya, M., & Jen, A. K.-Y. (2007). Peptide-mediated surface-immobilized quantum dot hybrid nanoassemblies with controlled photoluminescence. Journal of Materials Chemistry, 17(9), 866–872. https://doi.org/10.1039/B615010A